Spectra Gap modulation for optimization of dual-energy CT performance on estimation of proton stopping power

D. Han, [1][*] S. Zhang[2][*] and K. Ding[1]
[1]Department of Radiation Oncology, Johns Hopkins University, Baltimore, MD U.S.A
[2]Department of Electrical Engineering, Washington University at St. Louis
[*]Authors contribute equally

JULY 12–16
2020 VIRTUAL
JOINT AAPM | COMP MEETING
EASTERN TIME [GMT-4]

INTRODUCTION

Dual-energy computed tomography (DECT) approach has shown great promise in the reduction of proton range uncertainties by accurately estimating stopping power (SP). The achieved accuracy on a commercial DECT scanner, where an image-domain method for estimating SP is implemented, suffers from image reconstruction errors and scanning conditions deviation from calibrations. Although it is suggested that the maximum spectra separation should be used, there is **no study on the effect of separation of two spectra on proton SP prediction accuracy via image-domain DECT imaging technique**, nor a theoretical framework that enables one to quantify the relationship between spectra separation and performance of predicting SP for end-to-end test using DECT scanner

AIM

- To seek the correlation between spectral overlap of the DECT scanner and SP estimation accuracy via image-domain method
- To determine the optimal pair of the spectra under different scanning conditions, i.e., phantom size dependent, via simulation

METHOD

- The low energy range is from 80 kVp to 100 kVp, and the high energy range is from 120 kVp to 150 kVp. In order to further increase the spectral separation, tin filters with thickness from 0.1 mm to 1.5 mm with increment of 0.1 mm are added to spectrum of 150 kVp. The spectra pair used in this study can be seen in fig.1.
- To test the dependence of simulated accuracy on the phantom size given a specific spectra pair, three sizes of virtual Gammex are simulated.
- The elemental compositions of the phantom inserts are either from vender's manual or ICRU standard tissue reports. The geometrical tested phantoms are shown in fig.2.
- The workflows of this method is demonstrated in fig.3. The image-domain DECT method can be found in Ref.1. No noise is added to the simulated projection data for reconstruction.
- The root-mean-squared-error (RMSE) of 34 ICRU standard tissue substitutes are reported
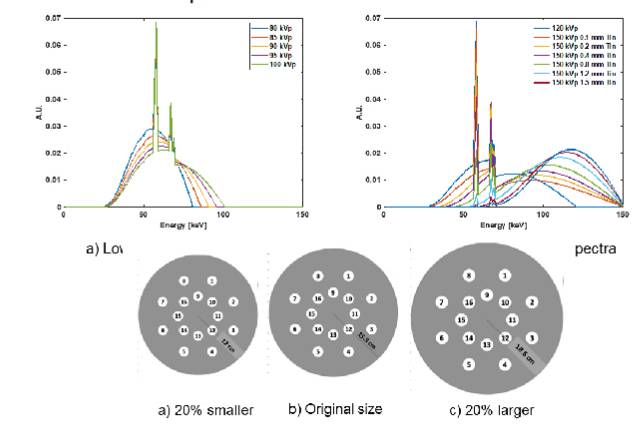

a) Low spectra

a) 20% smaller   b) Original size   c) 20% larger
Fig.2 Three sizes of synthetic Gammex phantom

RESULTS

- Depending on phantom size, the optimal DECT spectra for best SP prediction accuracy could be different. For example, instead of largest spectra 80 kVp and 150 kVp with 1.5 mm tin filter, for Gammex phantom size smaller than standard one, the spectra pair can yield the least accurate estimation is 80 kVp and 150 kVp with 0.4 mm tin filter. The RMSE of the investigated tissue inserts for 80 kVp and 150 kVp (0.4 mm tin) is 0.25%, while for the combination of 80 kVp and 150 kVp (11.5 mm tin), the corresponding error could be 0.64%. The RMSE distribution of each spectra pair is shown in fig. 4 and fig.5 for test phantom size 20% smaller than and equal to standard size of Gammex phantom.
- The relative SP errors of 34 ICRU standard human tissues are shown in fig.6 for the case of test phantom size 20% smaller than and equal to standard size of Gammex phantom Most of the tissues have SP accuracy about 0.5%. However, if the test phantom is 20% larger than standard size of Gammex phantom, the largest spectra separation 80 kVp and 150 kVp (1.5 mm) can estimate SP with lowest error of 0.27% among all the possible spectral pairs.

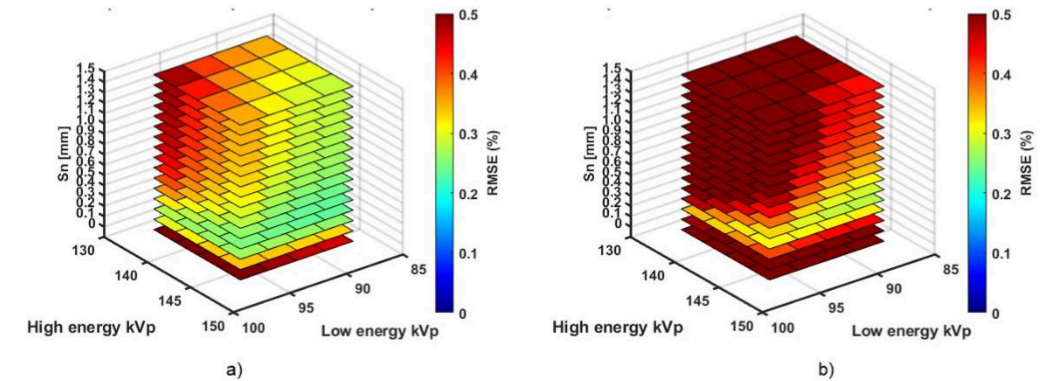a)   b)

Fig. 4 RMSE of SP distribution of all investigated low and high energy spectra, with thickness of filter shown in z-axis in the case of a) test phantom is 20% smaller b) test phantom is equal to standard size of Gammex phantom

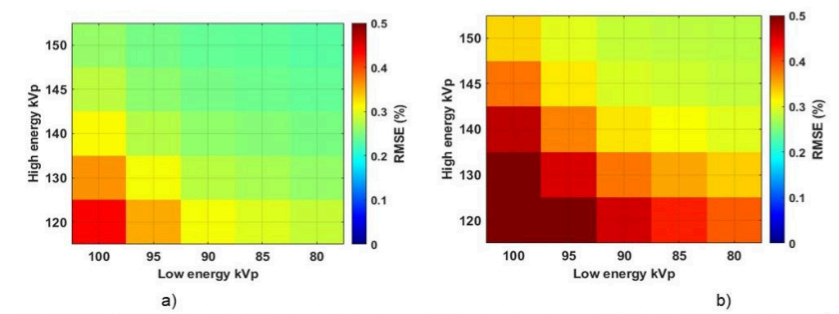a)   b)

Fig. 5 RMSE SP distribution of investigated low and high energy spectra with the tin filter thickness of 0.4 mm and 1.5 mm in the case of a) test phantom is 20% smaller b) test phantom is equal to standard size of Gammex phantom
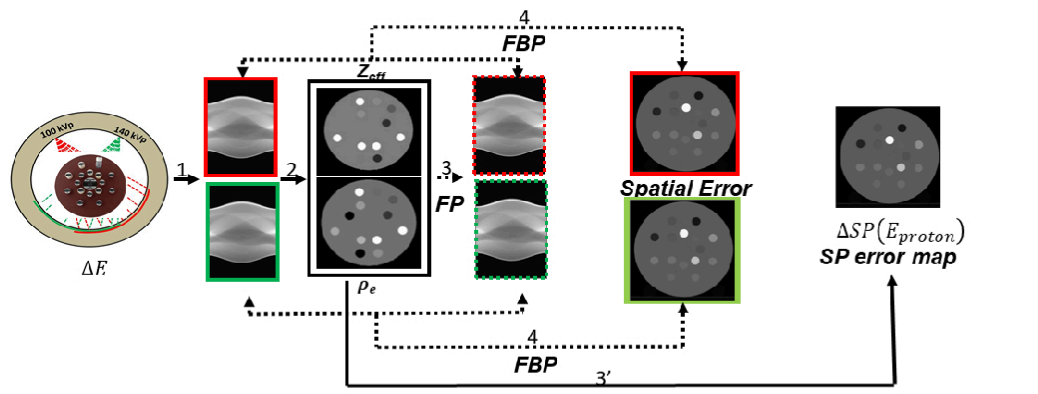

Fig.3 The flowchart of correlation of spectral pair and SP prediction error. The low and high energy projection or images are shown in red and green; step 1: simulation or experimental acquisition of projection data; step 2: reconstruction and decomposition from images to Z_{eff} and ρ_e maps; step 3: Using $f(\rho_e, Z_{eff}, E)$ to simulate the forward projection for two spectra; step 3': Using the maps of Z_{eff} and ρ_e to compute SP map and compare with the ground truth to obtain the $\Delta SP(E_{proton})$; step 4: Spatial error maps are from reconstruction of projection error using FBP algorithm
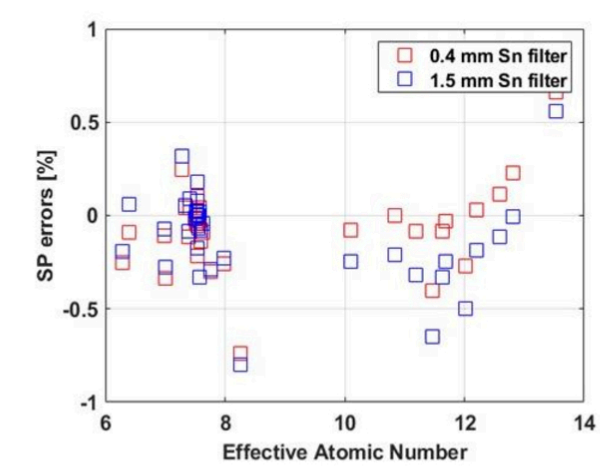

Fig. 6 SP relative error of 34 ICRU standard tissues comparison between 80kVp/150kVp (0.4 mm Sn filter) a) test phantom is 20% smaller than standard Gammex phantom

CONCLUSIONS

A series of spectral gap scenarios are employed to assess the vulnerability of image-domain method of predicting SP accuracy under the. It is also found that the 80 / 140 kVp with 0.4 mm tin filter spectral pair can yield the most accurate SP prediction for phantom size 20% less standard calibration one. This theoretical simulation study indicates that

- The choice of energy pair be optimized to achieve the most quantitative accuracy of predicting SP in clinical application of proton therapy, in other words, the maximum spectrum gap may not always yield the most accurate estimation.

- One of the reasons can be attributed to is the beam hardening effect, which can cause artifacts of CT number variations in images if not appropriated accounted. For smaller test phantom, the preprocessing steps prior to reconstruction step, may have sufficiently accounted for beam hardening effect, thus, the largest spectral gap may not necessarily lead to the most accurate the SP predictions.

- The spectra gap may need careful design to achieve the desired estimation accuracy if the size difference between calibration and test phantom is observed.

REFERENCES

1.Hünemohr N, Krauss B, Dinkel J, Gillmann C, Ackermann B, Jäkel O and Greilich S 2013 Ion range estimation by using dual energy computed tomography Z. Med. Phys. 23 300–13 Online: http://dx.doi.org/10.1016/j.zemedi.2013.03.001

2. Hünemohr N, Krauss B, Tremmel C, Ackermann B, Jäkel O and Greilich S 2014 Experimental verification of ion stopping power prediction from dual energy CT data in tissue surrogates Phys. Med. Biol. 59 83–96 Online: http://stacks.iop.org/0031-9155/59/i=1/a=83?key=crossref.8816994b2b96a7f29939baae0c5b34bb5

3. Li B, Lee H C, Duan X, Shen C, Zhou L, Jia X and Yang M 2017 Comprehensive analysis of proton range uncertainties related to stopping-power-ratio estimation using dual-energy CT imaging Phys. Med. Biol. 62 7056–74 Online: https://doi.org/10.1088/1361-6560/aa7dc9

4. Zhang S, Han D, Politte D G, Williamson J F and O'Sullivan J A 2018b Impact of joint statistical dual-energy CT reconstruction of proton stopping power images: Comparison to image- and sinogram-domain material decomposition approaches Med. Phys. 45 2129–42

5. Zhang S, Han D, Williamson J F, Zhao T, Politte D G, Whiting B R and O'Sullivan J A 2019 Experimental implementation of a joint statistical image reconstruction method for proton stopping power mapping from dual-energy CT data Med. Phys. 46 273–85